

Remote Sensing-Based Assessment of Glacier Change in Hunza Valley Using Google Earth Engine and NDSI Approach

Moaz Zafar¹, Basir Ali¹, Daud Khan^{2*}, Zeenat Khan³ and Abdullah Ikram⁴

¹Department of Geography and Geomatics, University of Peshawar, Peshawar, Pakistan.

²Resident Engineer, Al-Mussawwir Engineering, Rawalpindi, Pakistan.

³Research Analyst, Al-Mussawwir Engineering, Rawalpindi, Pakistan.

⁴Project Director, Al-Mussawwir Engineering, Rawalpindi, Pakistan.

*Correspondence:

Daud Khan, Resident Engineer, Al-Mussawwir Engineering, Rawalpindi, Pakistan.

Received: 06 Apr 2026; **Accepted:** 03 May 2026; **Published:** 11 May 2026

Citation: Moaz Zafar, Basir Ali, Daud Khan, et al. Remote Sensing-Based Assessment of Glacier Change in Hunza Valley Using Google Earth Engine and NDSI Approach. Insights Sci Technol. 2026; 1(1): 1-14.

ABSTRACT

This study investigates the spatio-temporal changes in glacier extent in the Hunza District, Gilgit-Baltistan, Pakistan, over a ten-year period from 2015 to 2025. Utilizing Google Earth Engine (GEE), multi-temporal satellite imagery from Landsat and Sentinel missions was processed to evaluate glacier dynamics using the Normalized Difference Snow Index (NDSI). The analysis focused on four major glaciers: Batura, Passu, Gulmit, and Ghulkin. Results indicate a consistent reduction in glacier area across all study sites, with Batura Glacier decreasing from 420 km² to 409 km², Passu from 60.9 km² to 60.6 km², Gulmit from 17.1 km² to 16.9 km², and Ghulkin from 26.8 km² to 25.5 km². The observed glacier retreat shows a strong association with rising regional temperatures and variable precipitation patterns derived from NASA POWER climate data. Spatial analysis further revealed that lower elevation zones are more susceptible to glacier melt, while topographic factors such as elevation, slope, and aspect significantly influence glacier stability and resilience. These findings highlight the importance of continuous monitoring of glacier dynamics in northern Pakistan due to their direct implications for freshwater availability, agriculture, and hydropower resources. The study demonstrates the effectiveness of Google Earth Engine as a robust platform for large-scale cryospheric monitoring and provides valuable insights into climate-driven glacier changes in high mountain environments. Climatic analysis indicates that glacier loss is closely linked to regional temperature increase and irregular precipitation trends. NASA POWER data show that mean annual temperature increased from 25.5°C in 2015 to 31°C in 2025, while precipitation exhibited temporal variability with an overall declining trend toward the end of the study period. These climatic changes contributed to accelerated glacier melting, particularly in low-elevation zones between 2800–3500 meters, where exposure to solar radiation intensifies ablation processes. Topographic assessment using SRTM-based digital elevation models further confirms that elevation, slope, and aspect play a crucial role in controlling glacier response, with north-facing slopes exhibiting comparatively lower rates of retreat due to reduced solar radiation exposure.

Keywords

Glacier Retreat, Spatio-Temporal Analysis, Google Earth Engine, NDSI, Hunza Glacier, Remote Sensing, Climate Change.

Highlights

- Multi-temporal satellite data used to map glacier changes from 2015–2025

- All four glaciers show consistent area reduction linked to rising temperature
- Google Earth Engine proved effective for large-scale cryospheric monitoring

Introduction

Glaciers represent the largest terrestrial reservoir of freshwater

on Earth and play a fundamental role in sustaining regional and global hydrological systems [1]. Mountain glaciers regulate river discharge by storing solid precipitation during cold seasons and releasing meltwater during warmer periods, ensuring a continuous freshwater supply for agriculture, ecosystems, and human consumption [2]. In recent decades, glaciers across the world have been retreating at unprecedented rates due to rising global temperatures, making them highly sensitive indicators of climate variability and long-term environmental change [3]. This accelerated cryospheric loss has raised serious concerns regarding freshwater security, sea level rise, and the stability of high-mountain hydrological systems [4]. Glacier and seasonal snow cover are widely recognized as key indicators of regional climate variability because they respond rapidly to changes in temperature and precipitation patterns [5]. Increasing frequency of heatwaves, prolonged warm seasons, and shifting precipitation regimes have further intensified glacier melt, particularly in arid and semi-arid mountain regions [6]. These processes contribute to reduced long-term water availability and increased hydrological uncertainty for downstream populations [7]. Glacier retreat also disrupts ecological systems by altering sediment transport, river flow regimes, and aquatic habitats [8]. In addition, it increases the likelihood of natural hazards such as glacial lake outburst floods, which pose severe risks to mountain communities [9]. Therefore, systematic monitoring of glacier dynamics is essential for understanding climate impacts and supporting sustainable water resource management strategies [10]. Global glacier decline represents a critical environmental challenge with far-reaching hydrological and ecological consequences.

Pakistan is among the most glacier-dependent countries outside the polar regions, where the cryosphere plays a central role in national water security and socioeconomic development [11]. The Indus River system, which is the lifeline of the country, derives a significant portion of its annual runoff from snow and glacier melt originating in the northern high mountain ranges [12]. The Upper Indus Basin contributes nearly half of the annual water discharge through combined snow and glacier-fed hydrological processes, making it highly sensitive to climatic fluctuations [13]. This basin forms part of the Hindu Kush, Karakoram, and Himalaya (HKH) mountain system, which contains one of the largest concentrations of mid-latitude glaciers globally [14]. These glacier systems are crucial for sustaining irrigation networks, hydropower production, drinking water supplies, and rural livelihoods in downstream regions [15]. However, recent climate change has led to increased atmospheric temperatures and altered precipitation patterns, accelerating glacier retreat across the HKH region [16]. This rapid cryospheric decline has intensified concerns regarding seasonal water variability, long-term water scarcity, and hydrological extremes such as floods and droughts [17]. The reduction in glacier mass also threatens agricultural productivity by destabilizing irrigation-dependent farming systems [18]. Furthermore, increased glacier melt contributes to the formation and expansion of glacial lakes, raising the risk of outburst floods [19]. As a result, glacier monitoring in this region is critical for water resource planning

and disaster risk reduction [20]. The HKH cryosphere is a vital but increasingly vulnerable component of regional water and climate systems.

The northern mountainous region of Pakistan hosts some of the world's highest peaks, including K2, Nanga Parbat, and Tirich Mir, which support extensive and diverse glacier systems [21]. These glaciers cover an estimated area of approximately 15,000 km² and include multiple glacier types such as valley, cirque, hanging, ribbon, and compound valley glaciers [22]. Among the most significant glacier systems in the region are the Siachen, Biafo, and Baltoro glaciers, which are among the largest glaciers outside the polar regions in terms of spatial extent and ice volume [23]. These glacier systems serve as major contributors to the Hunza and Nagar river networks, which ultimately feed into the Indus River basin [24]. The region is characterized by a cold-arid climate with strong altitudinal variations in temperature and precipitation, while overall rainfall remains relatively low [25]. Such climatic conditions make glacier mass balance highly sensitive to even small changes in temperature and precipitation regimes [26]. The rugged topography further enhances spatial variability in glacier behavior and melt patterns across short distances [27]. Because of these factors, the region is highly vulnerable to climate-induced glacier changes and associated hydrological impacts [28]. Continuous observation of glacier dynamics is therefore necessary for assessing environmental change and water resource sustainability in high mountain systems [29]. This also provides a foundation for evaluating long-term climate impacts on cryospheric stability in the region [30]. The complex Himalayan–Karakoram–Hindu Kush topography makes glacier systems highly dynamic and highly sensitive to climatic variation.

Advancements in geospatial science have significantly improved the capacity to monitor glacier dynamics across remote and inaccessible mountain regions [31]. Cloud-based platforms such as Google Earth Engine provide large-scale computational infrastructure for processing and analyzing geospatial datasets efficiently [32]. These systems integrate multi-petabyte satellite data archives with high-performance parallel computing capabilities, enabling time-series analysis over extended temporal scales [33]. The platform provides access to preprocessed satellite imagery from optical and radar sensors, which is essential for detecting changes in glacier extent and surface characteristics [34]. Such capabilities reduce computational barriers and allow researchers to perform large-area environmental monitoring with high temporal resolution [35]. This makes it particularly suitable for studying cryospheric changes in high-altitude regions where field access is limited and data collection is challenging [36]. The current study focuses on the Upper Hunza Valley in District Hunza Nagar, Gilgit Baltistan, Pakistan, a high-altitude region strongly influenced by glacier-fed hydrological systems. The study area lies between 73°59'E to 76°00'E longitude and 35°55'N to 36°51'N latitude and is geographically bounded by China, Afghanistan, and neighboring districts of Pakistan (Figure 1). The primary aim of this research is to analyze spatio-temporal changes in

selected glaciers of the Hunza region over the period 2015–2025 using satellite-based remote sensing techniques. The objectives include quantifying temporal variations in glacier extent and mapping spatial changes using multi-temporal satellite imagery processed through Google Earth Engine. This research contributes to improved understanding of cryospheric dynamics and supports sustainable water resource management and climate change adaptation in the region. The integration of remote sensing and cloud-based geospatial tools enables robust, large-scale glacier monitoring essential for long-term environmental assessment.

Literature Review

Glacier and snow cover dynamics in high mountain regions have been widely studied using multispectral satellite datasets to understand long-term cryospheric variability [1]. Certain high-altitude regions such as West Kunlun and Pamir have shown stable or slightly positive glacier mass balances despite the global trend of glacier recession [2]. MODIS-derived Normalized Difference Snow Index (NDSI) thresholding has been effectively used to extract annual snow and glacier cover for temporal trend analysis [3]. Landsat-5 TM and Landsat-8 OLI datasets are commonly used to validate MODIS-derived glacier mapping and reduce classification uncertainty [4]. Multi-temporal analysis across major subregions of the Tarim Basin has revealed heterogeneous glacier retreat patterns influenced by local climatic conditions [5]. The East Tien Shan region has exhibited the most rapid glacier decline

compared to other surrounding subregions [6]. Western subregions such as West Tien Shan and Pamir have experienced comparatively slower glacier reductions over multi-decadal periods [7]. Atmospheric circulation systems, particularly westerly winds, have been identified as a key factor influencing regional glacier stability [8]. Seasonal variability analysis shows that July to September provides optimal conditions for distinguishing permanent snow from seasonal snow cover [9]. Temporal snowmelt cycles play a critical role in separating transient snow from long-term glacier ice in remote sensing datasets [10]. Regional climatic circulation patterns strongly regulate spatial differences in glacier response to global warming [11]. These studies collectively demonstrate that glacier variability is strongly controlled by regional climatic and atmospheric circulation patterns.

Long-term Landsat time-series analysis has been widely applied to reconstruct glacier extent changes in tropical mountain regions [12]. Google Earth Engine provides a cloud-based platform that enables efficient processing of large-scale satellite datasets for glacier monitoring [13]. Digital image processing techniques combined with spectral band analysis are commonly used to improve glacier classification accuracy [14]. Temporal filtering methods are essential for reducing noise and ensuring consistency in multitemporal glacier datasets [15]. Significant glacier area loss has been observed in tropical glacier systems over the past several decades [16]. Elevation-dependent warming has been

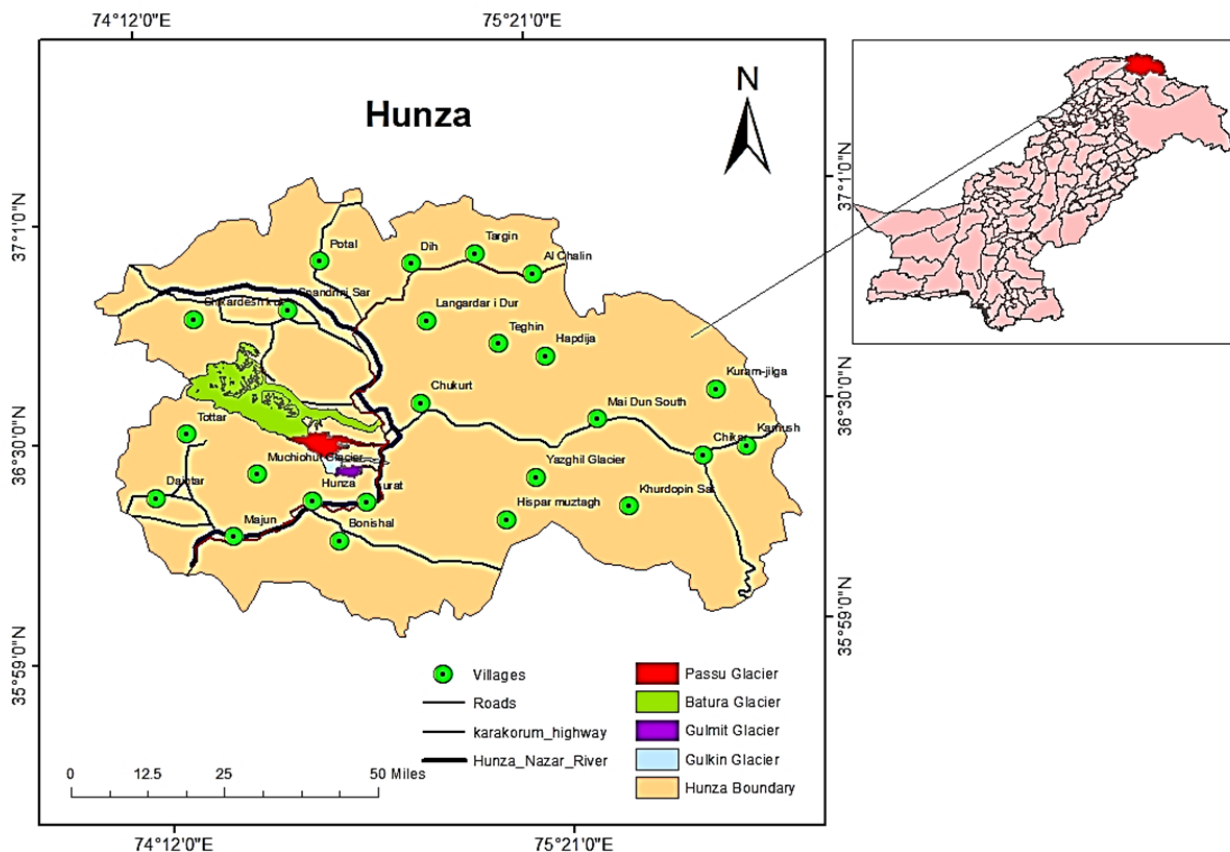


Figure 1: Location map of the study area (Hunza District, Northern Pakistan).

identified as a major driver of accelerated glacier retreat at lower altitudes [17]. Glacier loss patterns vary significantly with slope, latitude, and longitudinal gradients in mountainous terrain [18]. Smaller glacierized regions tend to experience higher percentage losses compared to larger glacier systems [19]. High classification accuracy values indicate the reliability of satellite-based glacier mapping approaches [20]. Tropical glaciers are highly sensitive indicators of climate change due to their rapid response to atmospheric warming [21]. These findings confirm that tropical glaciers are highly vulnerable and rapidly responding indicators of ongoing climate change.

Snow cover area monitoring in high mountain basins is essential for understanding regional water availability and hydrological processes [22]. Google Earth Engine-based analysis of Landsat imagery enables long-term monitoring of snow cover variability across complex terrains [23]. Normalized Difference Snow Index is widely used for delineating snow-covered areas in mountainous regions [24]. Elevation-based analysis using digital elevation models helps in understanding spatial distribution of snow cover [25]. Climatic datasets such as precipitation and temperature are essential for analyzing snow–climate interactions [26]. Increasing snow cover trends in some high-altitude basins have been linked to changes in precipitation and temperature regimes [27]. Contrasting snow cover behavior is often observed between lower and higher elevation zones within the same basin [28]. Climate variability produces complex and non-uniform responses in snow dynamics across mountain environments [29]. Snow cover changes are strongly influenced by local topographic and climatic heterogeneity [30]. Regional climate variability plays a dominant role in shaping snow accumulation and melt patterns [31]. These studies highlight that snow cover dynamics are highly variable and strongly controlled by elevation and local climate conditions.

Satellite-based glacier mapping in Arctic regions has enabled long-term assessment of cryospheric changes under warming conditions [32]. Object-based image analysis techniques improve the accuracy of glacier delineation in multispectral satellite imagery [33]. Multi-decadal glacier monitoring reveals consistent reductions in glacier area across Arctic coastal regions [34]. Spatial variability in glacier loss is strongly influenced by differences in regional warming intensity [35]. Coastal climatic conditions significantly affect the rate of glacier retreat in polar environments [1]. These results indicate that Arctic glacier systems are undergoing sustained and spatially variable retreat driven by differential regional warming patterns.

Machine learning algorithms integrated with cloud-based geospatial platforms have significantly improved glacier mapping accuracy [2]. Random forest classification has been identified as one of the most effective methods for glacier extraction in complex terrain [3]. Multi-source satellite data integration enhances spatial and temporal resolution in glacier monitoring studies [4]. Glacier retreat rates in mountain ranges show clear evidence of acceleration over recent decades [5]. Peripheral glacier zones and valley regions

are more vulnerable to rapid melting processes [6]. Summer temperature increase is a primary driver of accelerated glacier mass loss in high mountain environments [7]. High-resolution satellite datasets enable more precise monitoring of spatial variability in glacier change [8]. Temperature-driven processes dominate glacier evolution in many arid and semi-arid mountain basins [9]. Machine learning-based approaches provide improved classification accuracy for long-term glacier change detection [10]. These findings emphasize that advanced computational and machine learning approaches significantly enhance the precision of glacier monitoring and change detection.

Remote sensing combined with GIS techniques provides an effective framework for monitoring active glacier regions in complex mountainous terrain [11]. Glacierized regions in different mountain systems exhibit varying levels of sensitivity to climate change [12]. Normalized Difference Snow Index derived from satellite imagery is widely used for glacier and snow mapping applications [13]. Active glaciers serve as important indicators of regional and global climate change impacts [14]. Remote sensing approaches are essential for monitoring inaccessible glacier regions with high spatial complexity [15]. Glacier systems in mountainous regions respond rapidly to even small climatic variations [16]. GIS-based spatial analysis enhances understanding of glacier distribution and landform evolution [17]. Climate-sensitive glacier regions provide valuable evidence of ongoing environmental change [18]. Glacier monitoring using geospatial tools supports improved understanding of cryospheric dynamics [19]. Mountain glaciers act as early warning indicators of broader climatic shifts [20]. These studies confirm that geospatial technologies are essential tools for understanding and monitoring climate-driven glacier dynamics.

Climate variability analysis using statistical and time-series models provides important insights into regional environmental change [21]. Regression-based approaches help identify relationships between temperature and precipitation trends in mountain climates [22]. Time series models such as AR(1) are commonly used for short-term climate forecasting in data-scarce regions [23]. Temperature trends in mountainous regions often show an increasing pattern over time [24]. Precipitation patterns may exhibit decreasing or highly variable trends depending on local climatic conditions [25]. Climatic forecasting models are useful for early warning systems in hazard-prone regions [26]. Statistical modeling supports better understanding of climate–environment interactions in high-altitude areas [27]. Climatic variability has direct implications for hydrological and environmental risk assessment [28]. Predictive climate models assist in regional planning and disaster mitigation strategies [29]. Time-series analysis improves understanding of long-term climate dynamics in mountainous environments [30]. These studies demonstrate that statistical and predictive models are essential for understanding and forecasting climate variability in mountainous regions.

Automated algorithms for glacier snow line and equilibrium line

estimation have improved large-scale cryospheric monitoring capabilities [31]. Satellite-based classification of snow and ice enables calculation of key glaciological parameters over long time periods [32]. Snow cover ratio and snow line altitude are important indicators of glacier mass balance conditions [33]. Multi-glacier validation studies across different mountain regions improve the robustness of algorithm performance [34]. Classification uncertainties in satellite data arise due to cloud cover, shadow effects, and spectral limitations [35]. Post-2000 satellite data generally provide improved accuracy due to better spatial and temporal resolution [1]. Regional variability in glacier behavior influences the performance of automated snow line estimation models [2]. Optical satellite data integration enhances the reliability of large-scale glacier monitoring systems [3]. Automated glacier monitoring methods reduce reliance on field-based measurements in inaccessible terrain [4]. Remote sensing algorithms provide scalable solutions for global cryospheric analysis and monitoring [5]. These findings confirm that automated remote sensing algorithms provide reliable and scalable tools for glacier monitoring and cryospheric assessment.

Research Methodology

Software Utilized

This study employed an integrated set of geospatial and statistical software tools to ensure efficient data processing, spatial analysis, visualization, and documentation of results. Google Earth Engine (GEE) was used as the primary cloud-based geospatial platform for large-scale satellite image processing, enabling efficient analysis of multispectral datasets, land cover classification, glacier delineation, and temporal change detection. ArcMap 10.8, developed by Esri, was used for spatial analysis, map production, and visualization of glacier extents and hydrological features, providing advanced GIS tools for geoprocessing and spatial interpretation. Microsoft Excel was used for data organization, cleaning, tabulation, and statistical summarization of extracted glacier and climatic variables, ensuring structured dataset management for further analysis. Microsoft Word was used for documentation, reporting, and preparation of the research manuscript in a structured academic format. Together, these tools formed a comprehensive analytical framework for geospatial and environmental data processing.

Data Sources

The data used in this study were obtained from freely accessible remote sensing and meteorological databases to ensure reproducibility and reliability of results. Satellite imagery was acquired through Google Earth Engine, while climatic data were retrieved from NASA POWER data access services. These datasets provided consistent spatial and temporal coverage suitable for analyzing glacier dynamics and associated climatic influences in the study region.

Spatial Data Acquisition

Multi-temporal satellite imagery was used to analyze spatio-temporal glacier changes in the study area. The dataset included one Landsat image from 2015 and two Sentinel images from 2020

and 2025, resulting in a total of three primary observation time periods (Table 1). These images were selected based on cloud-free conditions and seasonal consistency to ensure comparability across years. All satellite datasets were accessed and processed through the Google Earth Engine platform, which facilitated efficient computation and standardized preprocessing of large geospatial datasets.

Table 1: Satellite imagery datasets used in the study.

S. No.	Acquisition Date	Sensor	Satellite	Spatial Resolution (m)
1	15-Aug-2015	OLI-TIRS (Operational Land Imager & Thermal Infrared Sensor)	Landsat-8	30
2	30-Aug-2020	MSI (Multispectral Instrument)	Sentinel-2	10
3	20-Aug-2025	MSI (Multispectral Instrument)	Sentinel-2	10

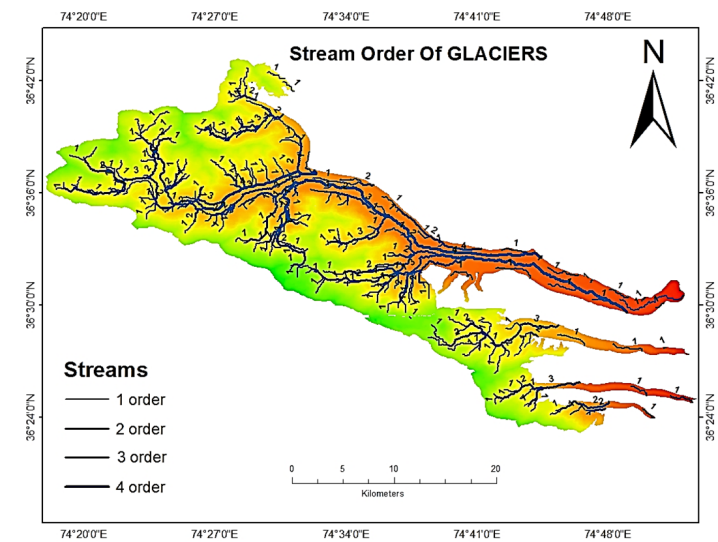


Figure 2: Stream Order of Glaciers.

Digital Elevation Model and Hydrological Analysis

A 30-meter resolution Shuttle Radar Topography Mission (SRTM) Digital Elevation Model (DEM) was obtained from Google Earth Engine for topographic and hydrological analysis (Figure 2). The DEM was used to derive terrain characteristics and extract stream networks within the study area. Arc Hydro tools in ArcMap 10.8 were applied to delineate catchment boundaries and analyze hydrological connectivity associated with major glacier systems, including Batura, Passu, Ghulkin, and Gulmit glaciers. This analysis supported the understanding of glacier-fed drainage patterns and watershed behavior in the region.

Meteorological Data Collection

Meteorological data, including temperature and precipitation records, were obtained from the NASA POWER data access platform. These datasets were used to assess climatic variability

and its potential influence on glacier dynamics within the study area. The climatic variables were aligned temporally with satellite observations to support comparative analysis between environmental conditions and observed glacier changes.

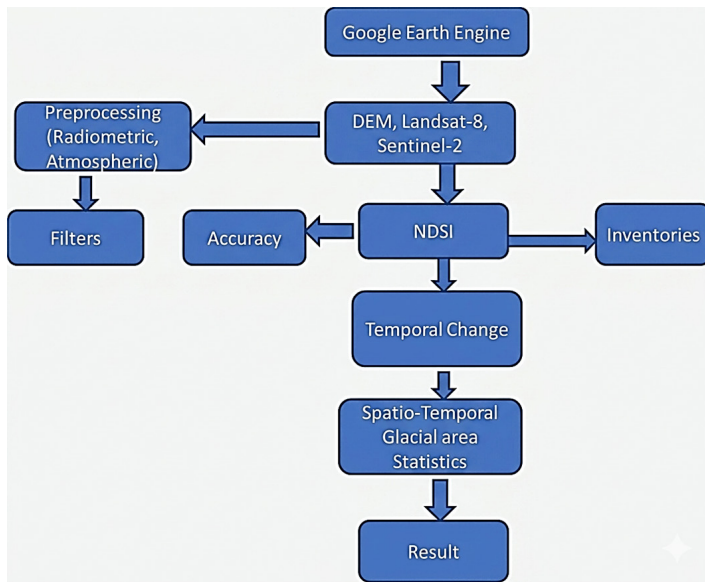


Figure 3: A methodological workflow for glacial area monitoring using Google Earth Engine. This process integrates multi-sensor satellite data (Landsat-8 and Sentinel-2) and uses the Normalized Difference Snow Index (NDSI) to calculate spatio-temporal glacial statistics.

Methodological Framework

The overall methodology was designed to detect and analyze spatio-temporal changes in glacier extent using remote sensing and GIS-based techniques. The workflow included data acquisition, preprocessing, glacier classification using spectral indices, accuracy assessment, and change detection analysis. Each stage was systematically implemented to ensure consistency, reliability, and reproducibility of results (Figure 3).

Data Preprocessing

Before analysis, all satellite imagery underwent preprocessing to improve data quality and ensure accurate classification results. Radiometric correction was applied to adjust sensor-related distortions and ensure that pixel values accurately represented surface reflectance. Atmospheric correction was performed to remove atmospheric interference such as haze, aerosols, and cloud effects. Additionally, cloud masking and quality filtering were applied to eliminate contaminated pixels and ensure only high-quality observations were used for analysis.

Normalized Difference Snow Index (NDSI) Based Glacier Extraction

The Normalized Difference Snow Index (NDSI) was used as the primary spectral index for identifying snow and glacier-covered areas. NDSI exploits the distinct reflectance characteristics of snow, which strongly reflects in the green band and absorbs in the shortwave infrared (SWIR) band. The index was computed

using the standard formula: $(Green - SWIR) / (Green + SWIR)$. Higher NDSI values indicate the presence of snow or glacier ice, while lower values represent non-snow land cover types such as vegetation, soil, or rock. This index is widely used in cryospheric studies for mapping snow distribution and detecting seasonal and long-term glacier changes.

```

    // Imports (4 entries)
    var table = Table projects/ee-moazkhattak161/assets/Batura
    var table2 = Table projects/ee-moazkhattak161/assets/Ghulkin
    var table3 = Table projects/ee-moazkhattak161/assets/Gulmit
    var table4 = Table projects/ee-moazkhattak161/assets/Passu

    1 // load glacier shapefiles from GEE assets
    2 var batura = ee.FeatureCollection('projects/ee-moazkhattak161/assets/Batura');
    3 var passu = ee.FeatureCollection('projects/ee-moazkhattak161/assets/Passu');
    4 var ghulkin = ee.FeatureCollection('projects/ee-moazkhattak161/assets/Ghulkin');
    5 var gulmit = ee.FeatureCollection('projects/ee-moazkhattak161/assets/Gulmit');
    6
    7 // Merge all glaciers into one FeatureCollection
    8 var glaciers = batura.merge(passu).merge(ghulkin);
    9
    10 // Define years for analysis
    11 var years = [2014, 2019, 2024];
    12
    13 // Function to get satellite data
    14 - function getSatelliteData(year) {
    15   var startDate = ee.Date.fromYMD(year, 8, 1);
    16   var endDate = ee.Date.fromYMD(year, 8, 31);
    17
    18   var collection;
    19   if (year === 2014) {
    20     collection = ee.ImageCollection('LANDSAT/LC08/C02/T1_TOA')
    21       .filterBounds(glaciers)
    22       .filterDate(startDate, endDate)
    23       .filter(ee.Filter.lt('CLOUD_COVER', 30));
    24   } else {
    25     collection = ee.ImageCollection('COPERNICUS/S2_SR')
    26       .filterBounds(glaciers)
    27       .filterDate(startDate, endDate)
    28       .filterDate(startDate, endDate)
    29       .filter(ee.Filter.lt('CLOUDY_PIXEL_PERCENTAGE', 30));
    30
    31   var image = collection.median().clip(glaciers);
    32   return ee.Algorithms.If(collection.size().gt(0), image, null);
    33 }
    34
    35 // Load NASA DEM
    36 var dem = ee.Image('USGS/SRTMGL1_003').clip(glaciers);
    37
    38 // Function to calculate NDSI
    39 function calculateNDSI(image, year) {
    40   return ee.Algorithms.If(
    41     image,
    42     ee.Image(image).normalizedDifference([year === 2014 ? 'B3' : 'B3', year === 2014 ? 'B6' : 'B11']),
    43     ee.Image('NDSI')
    44       .set('year', year),
    45     null
    46   );
    47 }
    48
    49 // Function to calculate glacier area in square kilometers
    50 function calculateGlacierArea(image, year) {
    51   return ee.Algorithms.If(
    52     image,
    53     ee.Feature(null, {
    54       'year': year, // Fix: Use 'year' directly
    55       'glacier_area_km2': ee.Number(
    56         ee.Image(image).gte(0.4).selfMask()
    57         .multiply(ee.Image.pixelArea()).reduceRegion({
    58           reducer: ee.Reducer.sum(),
    59           geometry: glaciers.geometry(),
    60           scale: 30,
    61           maxPixels: 1e13
    62         })),
    63       'NDSI'
    64     }),
    65     null
    66   );
    67 }
    68
    69 // Process each year
    70 var results = years.map(function(year) {
    71   var image = ee.Image(getSatelliteData(year));
    72   var ndsi = calculateNDSI(image, year);
    73   var glacierArea = calculateGlacierArea(ndsi, year);
    74
    75   // Export NDSI if valid
    76   if (ndsi) {
    77     Export.image.toDrive({
    78       image: ee.Image(ndsi),
    79       description: 'NDSI_' + year,
    80       folder: 'GEE_Export',
    81       fileNamePrefix: 'NDSI_' + year,
    82       scale: 30,
    83       region: glaciers.geometry(),
    84       maxPixels: 1e13,
    85       crs: 'EPSG:4326'
    86     });
    87   }
    88
    89   // Export Glacier Area Data if valid
    90   if (glacierArea) {
    91     Export.table.toDrive({
  
```

```

88 // Export Glacier Area Data if valid
89 if (glacierArea) {
90   Export.table.toDrive({
91     collection: ee.FeatureCollection(glacierArea),
92     description: 'Glacier_Area_' + year,
93     folders: 'GEE_Exports',
94     fileNamePrefix: 'Glacier_Area_' + year,
95     fileFormat: 'CSV'
96   });
97 }
98
99 // Fix: Check if glacierArea is not null before printing
100 glacierArea.evaluate(function(feature) {
101   if (feature) {
102     print('Glacier Area for ' + year + ' (sq km):', feature.properties.glacier_area_km2);
103   } else {
104     print('No valid glacier area data for ' + year);
105   }
106 });
107
108 return ndsi;
109 });
110
111 // Convert to ImageCollection
112 var ndsiCollection = ee.ImageCollection(results).filter(ee.Filter.notNull(['year']));
113
114 // Export SRTM DEM data to Google Drive
115 Export.image.toDrive({
116   image: dem,
117   description: 'SRTM_DEM',
118   folder: 'GEE_Exports',
119   fileNamePrefix: 'SRTM_DEM',
120   scale: 30,
121   region: glaciers.geometry(),
122   maxPixels: 1e10,
123   crs: 'EPSG:4326'
124 });
125
126 // Visualization
127 Map.centerObject(glaciers, 9);
128 var ndsiVis = { min: 0, max: 1, palette: ['black', 'blue', 'cyan'] };
129 years.forEach(function(year) {
130   var img = ndsiCollection.filter(ee.Filter.eq('year', year)).first();
131   if (img) Map.addLayer(img, ndsiVis, 'NDSI ' + year);
132 });
133
134 Map.addLayer(dem, { min: 0, max: 6000, palette: ['blue', 'green', 'yellow', 'red'] }, 'SRTM DEM');

```

Figure 4: Google Earth Engine workflow used for glacier extraction and analysis based on NDSI and SRTM datasets for estimating glacier extent in Batura, Passu, Ghulkin, and Gulmit glaciers (2015–2025).

Accuracy Assessment

The accuracy of glacier classification results was evaluated using a confusion matrix approach. Classified NDSI-based glacier maps were compared with reference data to determine the correctness of pixel classification. The confusion matrix provided information on correctly and incorrectly classified pixels across different land cover categories. This method enabled assessment of classification reliability and identification of potential errors in glacier delineation.

Overall Accuracy Evaluation

Overall classification accuracy was calculated as the ratio of correctly classified pixels to the total number of reference pixels. This metric provided a quantitative measure of the performance of the glacier classification model. Higher accuracy values indicated better agreement between classified outputs and reference data, confirming the reliability of the remote sensing-based glacier extraction method.

Implementation in Google Earth Engine

The entire analytical workflow was implemented using Google Earth Engine scripting environment. The code was designed to process Landsat and Sentinel imagery, apply NDSI-based classification, and integrate SRTM-derived elevation data for spatial analysis

(Figure 4). The processed outputs were used to estimate glacier extent changes in Batura, Passu, Ghulkin, and Gulmit glaciers over the study period from 2015 to 2025. This integrated approach enabled efficient, large-scale, and reproducible analysis of glacier dynamics using cloud-based geospatial technology.

Table 2: Comparison of glacier area changes from 2015–2025 for Batura, Passu, Gulmit, and Ghulkin glaciers.

Glacier	Area (km ²) 2015	Area (km ²) 2020	Area (km ²) 2025	Glacier Area Loss (km ²) (2015–2025)	Glacier Area Loss (%) (2015–2025)
Batura	420	418	409	11	2.61
Passu	64.9	63.9	60.6	4.3	6.62
Gulmit	17.1	16.8	16.9	0.2	1.2
Ghulkin	26.8	25.5	25.5	1.3	4.85

Results and Discussion

Glacier Inventory Map

The free availability of Landsat-8 and Sentinel-2 satellite archives enabled the assessment of spatio-temporal glacier changes from 2015 to 2025. The calculated glacier areas for Batura, Passu, Gulmit, and Ghulkin glaciers are presented in Table 2. Overall, all four glaciers exhibited a consistent decrease in area over the study period (Table 2). The area of the Batura Glacier decreased from 420 km² in 2015 to 418 km² in 2019 and further to 409 km² in 2025, indicating a total loss of 11 km² over the study period. This reduction shows a clear association between glacier retreat and rising temperature trends. Climatic data obtained from NASA POWER indicate that mean temperature increased from 25°C in 2015 to 31°C in 2025, while precipitation decreased from 186.89 mm in 2015 to 110 mm in 2025. These climatic changes strongly suggest that enhanced melting and reduced accumulation contributed to glacier mass loss. Historical variability in the Batura Glacier also confirms its sensitivity to temperature-driven fluctuations.

The Passu Glacier showed a reduction in area from 64.9 km² in 2015 to 63.9 km² in 2019 and further to 60.6 km² in 2025. This corresponds to a total area loss of 4.3 km² over the study period. The observed retreat is strongly linked with increasing air temperature and decreasing precipitation trends recorded in the region. The NASA POWER dataset indicates a temperature increase from 25°C in 2015 to 31°C in 2025, along with declining precipitation levels. Compared to Ghulkin Glacier, the Passu Glacier experienced a higher rate of retreat due to its relatively clean-ice surface exposure. Direct solar radiation exposure enhanced surface melting, accelerating mass loss in comparison to debris-covered glaciers. These findings highlight the strong influence of surface characteristics on glacier response to climatic forcing.

The Ghulkin Glacier showed a gradual reduction in area over the study period from 2015 to 2025 (Table 2). A decrease of 1.3 km² was observed between 2015 and 2019, while no significant change was detected between 2019 and 2025. The total net loss over the study period remained limited compared to other glaciers

in the region. The relatively slower rate of change is attributed to the presence of thick debris cover on the glacier surface, which reduces direct solar radiation impact. In contrast, cleaner glacier surfaces tend to respond more rapidly to atmospheric warming. When compared with Passu Glacier, the rate of retreat in Ghulkin Glacier is significantly lower, confirming the insulating effect of debris cover. These results demonstrate the importance of surface conditions in controlling glacier melt dynamics.

The Gulmit Glacier exhibited a reduction in area from 17.1 km² in 2015 to 16.1 km² in 2025 (Table 2). Although the total area loss is relatively small, it indicates a consistent long-term retreat trend. The limited magnitude of change is primarily due to the small size of the glacier compared to larger valley glaciers in the region. Similar to other debris-covered glaciers in the study area, the rate of retreat is comparatively slower. The insulating effect of debris cover reduces the direct impact of rising temperature on glacier ice. Despite the smaller absolute change, the persistent reduction indicates ongoing glacier sensitivity to climatic variability. These findings highlight that even small glaciers are gradually responding to regional warming trends.

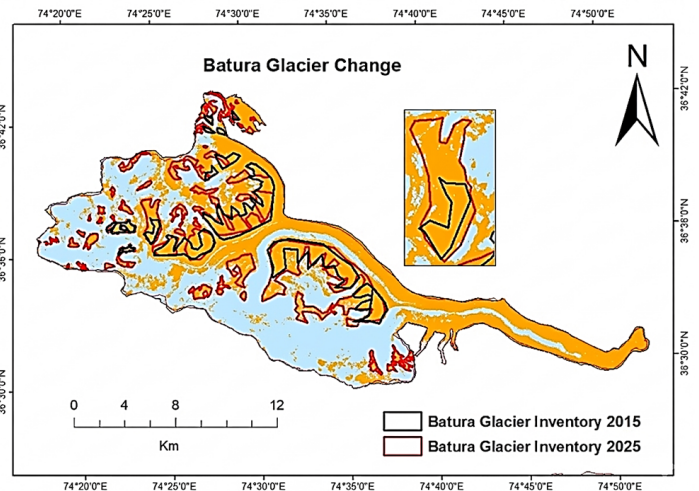


Figure 6: The Batura glacier decline between 2015-2025 NDSI. Black color shows the Baura glacier outline in 2015, red color shows the Batura glacier outline in 2025.

Batura Inventory Derived by Geo-Spatial Techniques

Glacier inventories were generated for each available NDSI-derived satellite image to analyze temporal changes in glacier

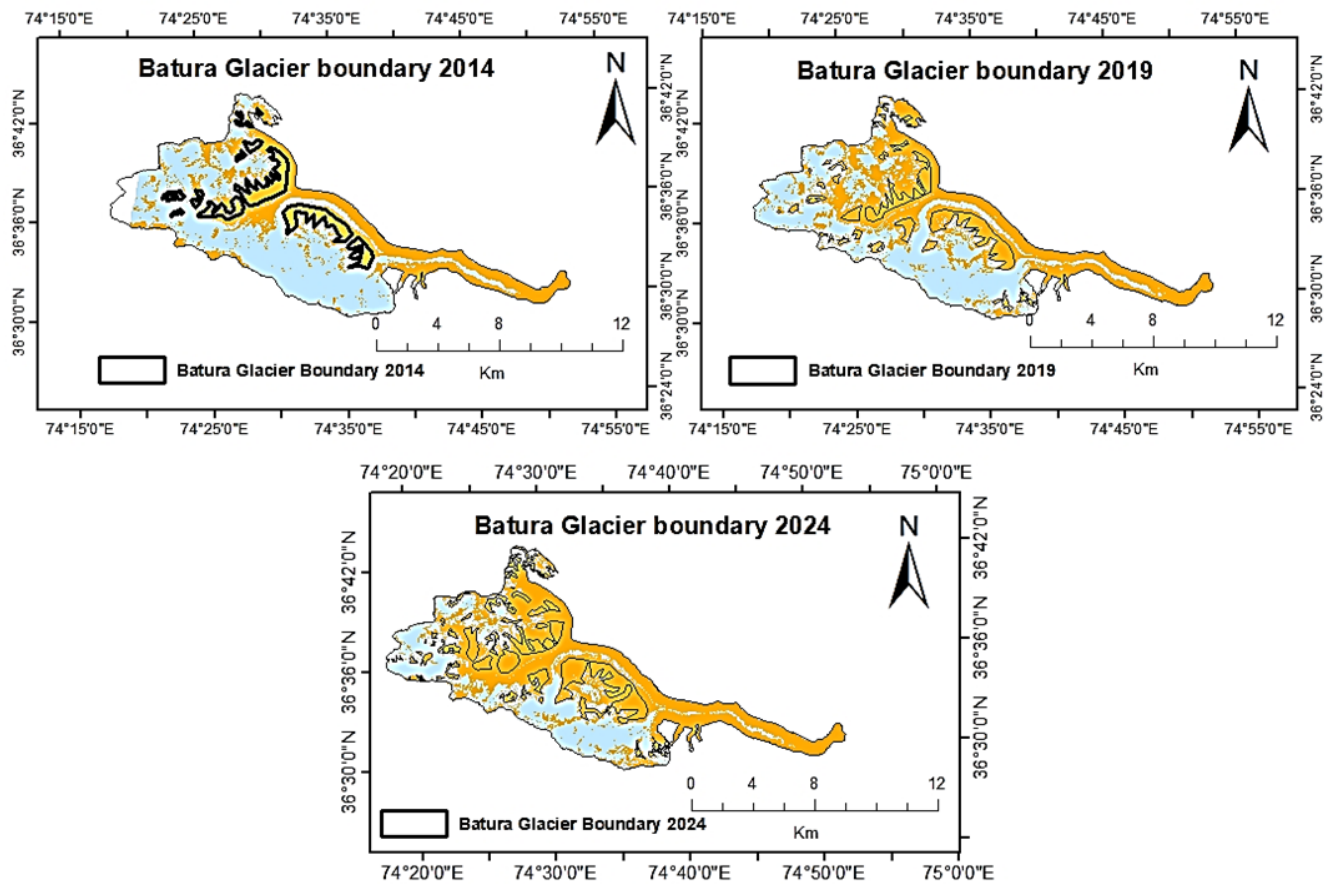


Figure 5: Three inventories of the Batura glacier from 2015-2025, shown on (SENTINEL-2, 2024 image, MSI sensor). Black line show glacier boundary extracted by techniques like NDSI. Manual digitization from Google Earth.

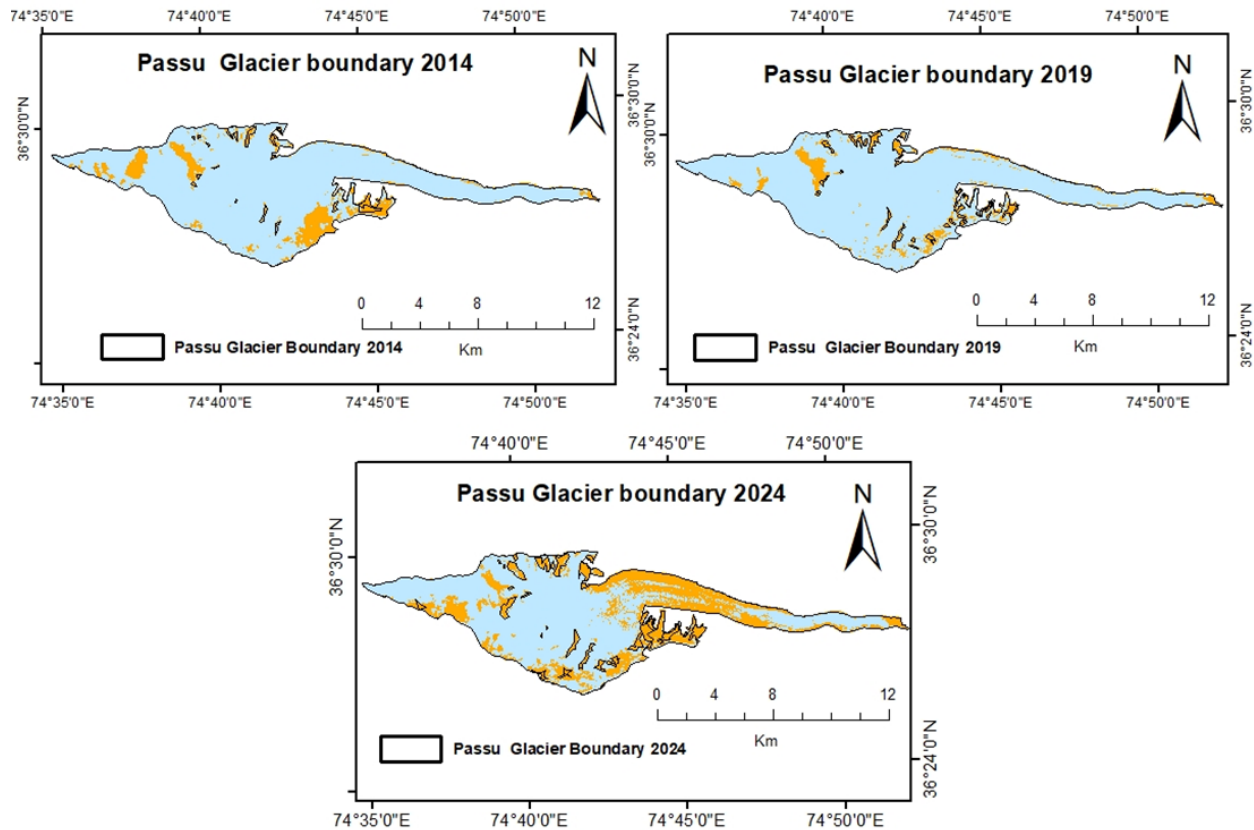


Figure 7: Three inventories of the Passu glacier from 2015-2025, shown on (SENTINEL-2, 2025 image, MSI sensor). Black line show glacier boundary extracted by techniques like NDSI. Manual digitization from Google Earth.

extent. Three separate inventories were prepared for the Batura Glacier covering the period from 2015 to 2025 (Figure 5). Debris-covered glaciers present significant challenges for accurate boundary delineation due to spectral similarity between debris and surrounding terrain. As a result, identifying precise terminus changes in the lower glacier sections remains difficult. In contrast, clean-ice regions exhibit clearer spectral signatures, allowing more reliable detection of spatial change. In the case of Batura Glacier, terminus fluctuations were less distinct due to extensive debris cover at the glacier front. However, visible changes in clean ice zones confirm ongoing glacier retreat over time. These results demonstrate the limitations of spectral-based mapping in debris-dominated glacier environments.

Overlay of the Outlines for Change Detection in The Batura Glacier

An overlay analysis of glacier outlines was performed using black boundaries for 2015 and red boundaries for 2025 to assess spatial change in Batura Glacier (Figure 6). The comparison of outlines indicates that terminus retreat is not easily distinguishable in debris-covered zones due to surface masking effects. However, changes in clean-ice regions of the glacier are clearly visible and indicate measurable spatial reduction. The total calculated glacier area loss for Batura Glacier was 11 km² over the study

period. This confirms a continuous retreat trend despite spatial mapping limitations in debris-covered areas. The overlay results provide strong visual evidence of long-term glacier shrinkage. These findings reinforce the importance of multi-temporal spatial analysis for glacier change detection.

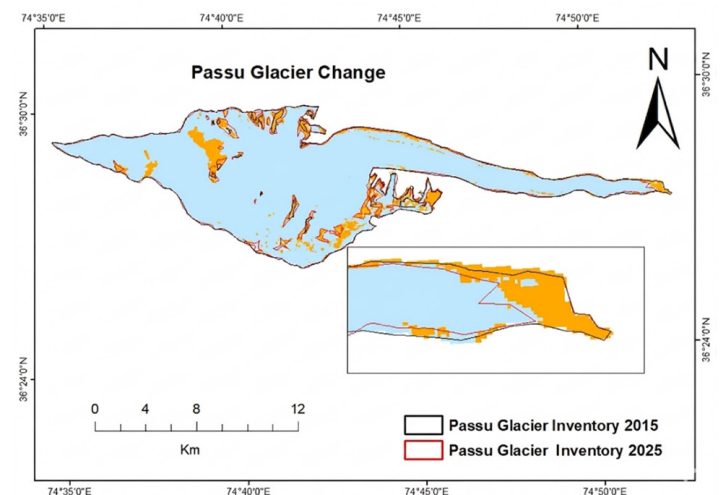


Figure 8: The Passu glacier decline between 2015-2025 NDSI. Black color shows the Passu glacier outline in 2015, red color shows the Passu glacier outline in 2025.

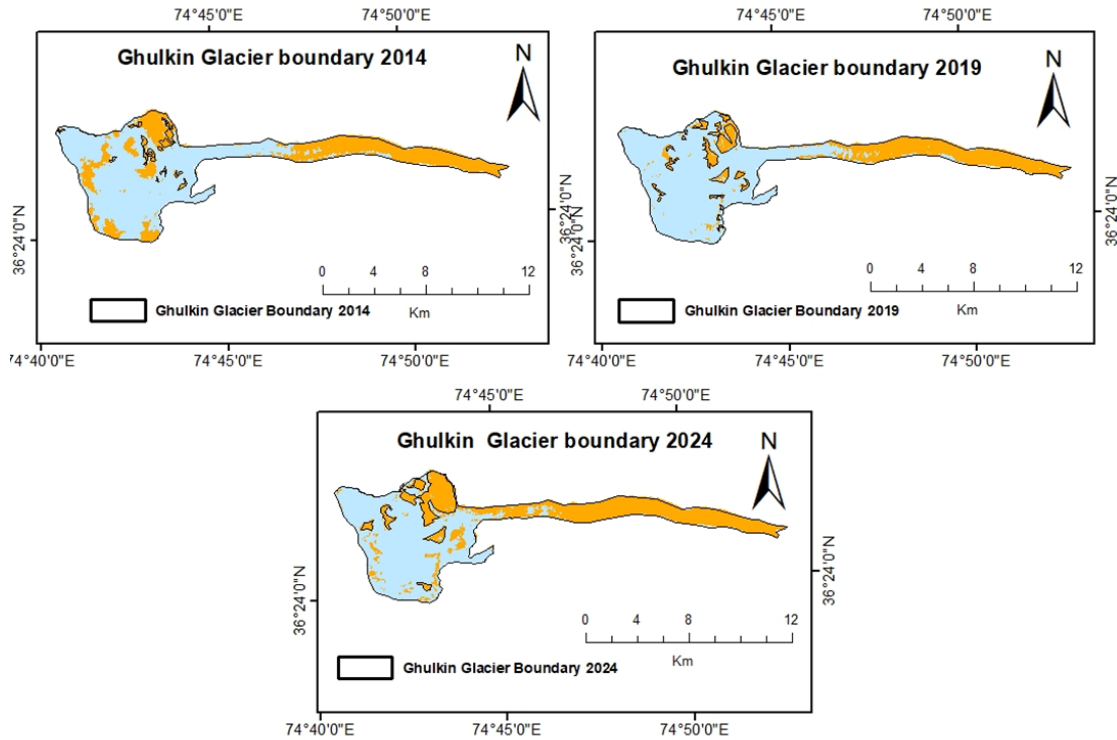


Figure 9: Three inventories of the Ghulkin glacier from 2015-2025, shown on (SENTINEL-2, 2025 image, MSI sensor). Black line show glacier boundary extracted by techniques like NDSI. Manual digitization from Google Earth.

Passu Inventory Derived by Geo-Spatial Techniques

Three glacier inventories were developed for Passu Glacier using NDSI-based satellite imagery covering the period from 2015 to 2025. An overlay of glacier outlines (black for 2015 and red for 2025) clearly illustrates the spatial retreat of the glacier terminus (Figure 7). Unlike debris-covered glaciers, Passu Glacier has a relatively clean-ice surface, allowing more precise detection of boundary changes. The terminus retreat is distinctly visible in the overlay comparison, confirming active glacier shrinkage (Figure 8). The total glacier area loss was calculated as 4.3 km² during the study period. These results indicate that Passu Glacier is highly responsive to climatic variations. The observed retreat pattern aligns with increasing temperature trends in the region.

Ghulkin Inventory Derived by Geo-Spatial Techniques

Three glacier inventories were generated for Ghulkin Glacier using multi-temporal satellite datasets from 2015 to 2025. The overlay of glacier outlines (black for 2015 and red for 2025) shows limited visible change at the glacier terminus (Figure 9). This is primarily due to extensive debris cover, which obscures clear boundary detection in optical imagery. As a result, terminus retreat is not distinctly observable despite measurable area changes. The total glacier area loss was estimated at 1.3 km² over the study period (Figure 10). Compared to clean-ice glaciers, the rate of retreat is significantly lower. These findings confirm that debris-covered glaciers exhibit reduced apparent surface change in remote sensing analysis.

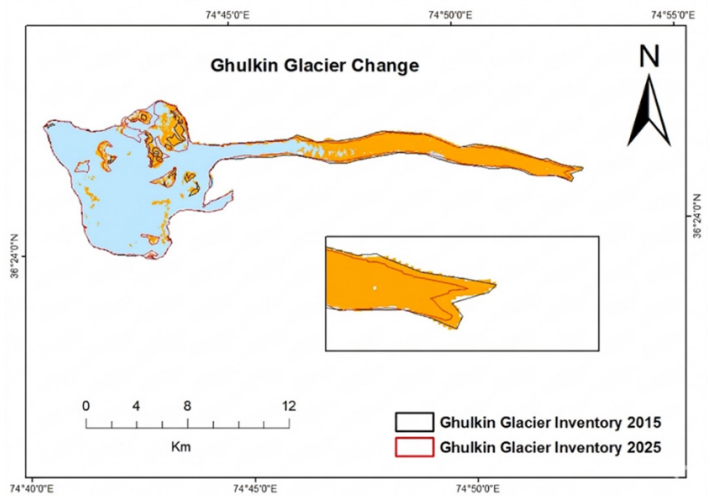


Figure 10: The Ghulkin glacier decline between 2015-2025 NDSI. Black color shows the Ghulkin glacier outline in 2015, red color shows the Ghulkin glacier outline in 2025.

Gulmit Inventory Derived by Geo-Spatial Techniques

Three glacier inventories were developed for Gulmit Glacier using satellite imagery spanning 2015 to 2025. The overlay comparison of glacier outlines shows minimal visible change in glacier boundaries due to debris cover effects. Similar to Ghulkin Glacier, the debris layer limits accurate detection of terminus variation in optical imagery (Figure 11). Despite this limitation, a

gradual reduction in glacier extent is observed over time. The total glacier area decreased from 17.1 km² to 16.1 km² during the study period. The rate of decline remains relatively slow compared to clean-ice glaciers in the region (Figure 12). These results suggest that debris-covered glaciers respond more gradually to climatic forcing, although long-term retreat is still evident.

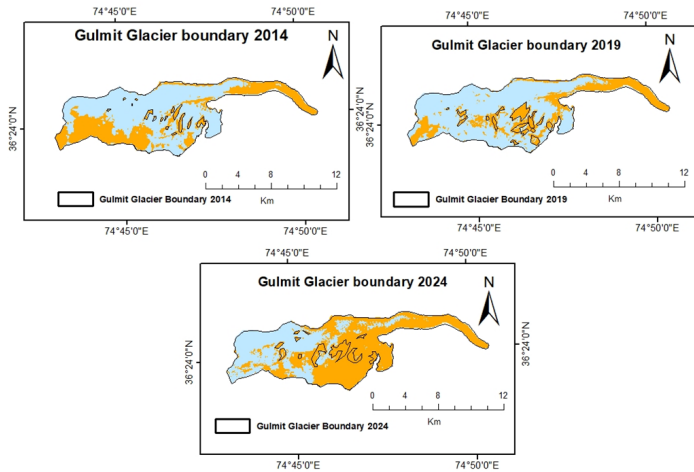


Figure 11: Three inventories of the Gulmit glacier from 2015-2025, shown on (SENTINEL-2, 2025 image, MSI sensor). Black line show glacier boundary extracted by techniques like NDSI. Manual digitization from Google Earth.

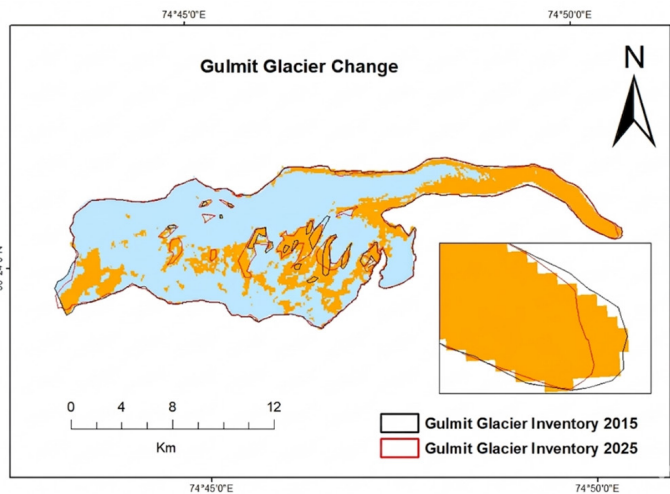


Figure 12: The Gulmit glacier decline between 2015-2025 NDSI. Black color shows the Gulmit glacier outline in 2015, red color shows the Gulmit glacier outline in 2025

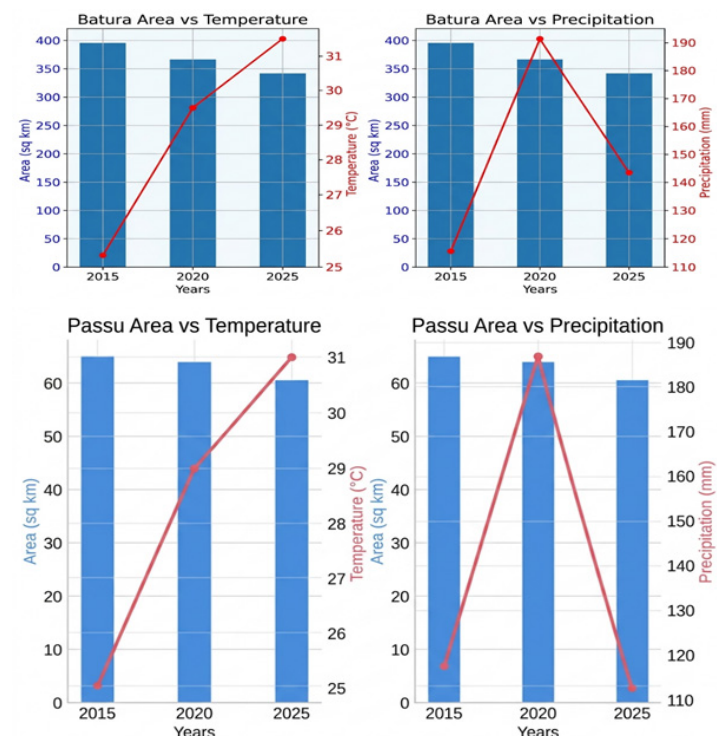
Statistical Analysis

The glacier area changes of Batura, Passu, Ghulkin, and Gulmit glaciers were statistically analyzed by correlating glacier extent with temperature and precipitation data to evaluate the influence of climatic variables on glacier dynamics. The analysis indicates a strong relationship between rising temperature, decreasing precipitation, and glacier area reduction over the study period. In

2025, the Batura Glacier had an area of 420 km² under relatively cooler conditions with a mean temperature of 25°C and higher precipitation of 186.89 mm. By 2025, the glacier area reduced to 409 km², corresponding with an increase in temperature to 31°C and a decline in precipitation to 110 mm over the study period. This clearly indicates that warming conditions combined with reduced moisture input contributed to enhanced glacier mass loss.

The Passu Glacier exhibited a decrease in area from 64.9 km² in 2015 to 60.6 km² in 2025, resulting in a total loss of 4.3 km². This reduction reflects a consistent retreat trend influenced by increasing regional temperature conditions. The Ghulkin Glacier showed a decline from 26.8 km² in 2015 to 25.5 km² in 2025, resulting in a total loss of 1.3 km² (Figure 13). This moderate reduction indicates a comparatively slower response to climatic forcing, largely due to the presence of debris cover which buffers direct melting effects. The Gulmit Glacier decreased from 17.1 km² in 2015 to 16.9 km² in 2025, with a total loss of 0.2 km².

The comparatively smaller magnitude of change in Gulmit Glacier is attributed to its limited spatial extent and debris-covered surface characteristics, which reduce direct exposure to solar radiation. In comparison, larger glaciers such as Batura and Passu show more pronounced area changes due to their higher sensitivity to atmospheric warming and surface exposure conditions. Although the absolute loss in smaller glaciers is lower, all four glaciers consistently exhibit a declining trend when correlated with increasing temperature and decreasing precipitation. These results confirm that climatic variability is the dominant driver of glacier retreat in the study area, with glacier size and surface characteristics controlling the rate of response.



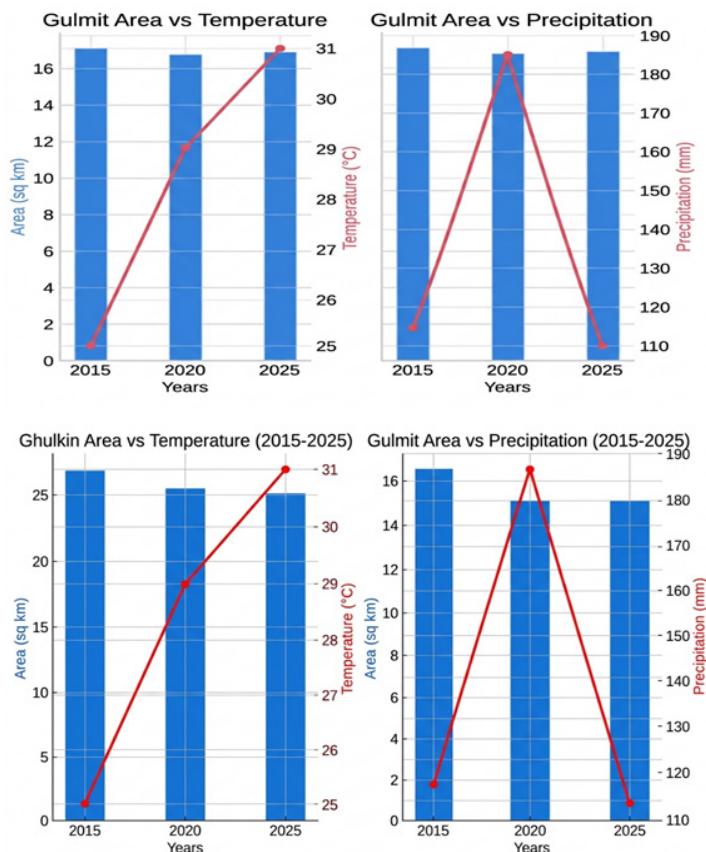


Figure 13: The Geographical representation of the Batura, Passu, Ghulkin and Gulmit glaciers area v/s precipitation and Temperature data from 2015 to 2025. From the below figures it is analyzed that both the variables (precipitation and glacier area) for each glacier area are directly proportional to each other i.e. Precipitation increase result in glacier area gain. On contrary, temperature and glacier are inversely proportional to each other i.e. temperature increase result in glacier area loss. Blue color show glacier area and Red color shows Temperature and Precipitation in the graph given below.

Discussion

The results of this study clearly demonstrate a consistent decline in glacier extent across the Upper Hunza region from 2015 to 2025, indicating a strong and ongoing response of the cryospheric system to climatic variability. The observed retreat in Batura, Passu, Ghulkin, and Gulmit glaciers is primarily driven by increasing air temperatures and decreasing precipitation, which together disrupt the glacier mass balance by enhancing ablation while reducing accumulation. The rise in temperature from 25°C to 31°C over the study period is a key controlling factor that intensified surface melting across all glaciers. However, the magnitude of glacier response varied significantly depending on glacier type and surface characteristics. Clean-ice glaciers such as Passu showed relatively higher retreat rates due to direct exposure to solar radiation, whereas debris-covered glaciers such as Ghulkin and Gulmit exhibited slower but still persistent area loss due to the insulating effect of supraglacial debris. These variations highlight that while climate forcing is the primary driver, local glacier

conditions strongly modulate the rate of response.

Spatial and statistical analyses further reinforce the strong link between glacier shrinkage and climatic trends, confirming that temperature increase combined with precipitation decline is accelerating glacier loss in the region. The overlay-based mapping results show that glacier terminus changes are more clearly detectable in clean-ice glaciers, whereas debris-covered glaciers present limitations in optical remote sensing due to spectral confusion between debris and surrounding terrain. Despite these challenges, multi-temporal satellite analysis using Landsat and Sentinel imagery effectively captured long-term glacier retreat patterns, demonstrating the reliability of remote sensing and Google Earth Engine for cryospheric monitoring in inaccessible mountainous regions. The statistical relationships between glacier area and climatic variables confirm a strong negative correlation, indicating that continued warming will likely intensify future glacier recession. Overall, these findings align with regional studies in High Mountain Asia and emphasize the urgent need for continuous monitoring, as glacier loss in the Upper Hunza region has direct implications for downstream water availability and long-term hydrological stability.

Conclusion

This study investigated the spatio-temporal changes in glacier extent in the Hunza region, Pakistan, using multi-temporal satellite imagery integrated with geospatial analysis in Google Earth Engine. Four major glaciers, including Batura, Passu, Ghulkin, and Gulmit, were analyzed over the period 2015 to 2025 to assess long-term changes in glacier dynamics. The results demonstrate a consistent and widespread reduction in glacier area across all selected glaciers, indicating a strong influence of regional climatic changes, particularly rising temperature and decreasing precipitation. The Batura Glacier experienced a total area loss of 11 km² (2.61%), while Passu Glacier lost 4.3 km² (6.62%). Similarly, Ghulkin Glacier showed a reduction of 1.3 km² (4.85%), and Gulmit Glacier exhibited a smaller decrease of 0.2 km² (1.2%). These findings confirm that glacier retreat is ongoing and varies significantly among glaciers depending on their size, elevation, and surface characteristics.

The comparative analysis further reveals that debris-covered glaciers such as Batura and Ghulkin exhibit relatively slower retreat rates compared to cleaner ice glaciers like Passu, where direct solar radiation exposure accelerates melting processes. The study also confirms that the Normalized Difference Snow Index (NDSI) is an effective tool for glacier delineation and monitoring in complex mountainous terrain, particularly when combined with high-resolution satellite datasets. Overall, the observed glacier decline highlights the increasing vulnerability of the Hunza cryospheric system to climate change. These results emphasize the urgent need for continuous glacier monitoring to support sustainable water resource management, reduce hydrological risks, and develop climate adaptation strategies in high-altitude regions where glacier meltwater plays a critical role in sustaining

downstream ecosystems and human livelihoods.

Acknowledgement

The authors would like to express their sincere gratitude to all individuals and departments who contributed to the successful completion of this research. Special thanks are extended to Al-Mussawwir Engineering and Creative Engineering Zone (CEZ) for their technical support and assistance throughout the study. The authors are also highly grateful to S.E. Hussain, Public Health Engineering Department Rawalpindi, for his valuable guidance and support.

References

1. Zhang J, Jia L, Menenti M, et al. Glacier area and snow cover changes in the range system surrounding Tarim from 2000 to 2020 using Google Earth Engine. *Remote Sensing*. 2021; 13: 5117.
2. Turpo Cayo EY, Borja MO, Espinoza- Villar R, et al. Mapping three decades of changes in the tropical Andean glaciers using Landsat data processed in the Earth Engine. *Remote Sensing*. 2022; 14: 1974.
3. Moazzam MFU, Rahman G, Lee BG, et al. Trend of snow cover under the influence of climate change using Google Earth Engine platform: A case study of Astore (Western Himalayas) and Shigar (Karakoram region). *Front Environ Sci*. 2022; 10: 1006399.
4. Ali A, Dunlop P, Coleman S, et al. Glacier area changes in Novaya Zemlya from 1986–89 to 2019–21 using object-based image analysis in Google Earth Engine. *Journal of Glaciology*. 2023; 69: 1305-1316.
5. Zhang Q, Zhang Z, Wang X, et al. Monitoring of glacier area changes in the Ili River Basin during 1992–2020 based on Google Earth Engine. *Land*. 2024; 13: 1417.
6. Zhuang L, Ke C, Cai Y, et al. Measuring glacier changes in the Tianshan Mountains over the past 20 years using Google Earth Engine and machine learning. *Journal of Geographical Sciences*. 2023; 33: 1939-1964.
7. Abdioğlu G, Kaya Y, Polat N. Calculation of glacial area change at Cilo Mountain with Google Earth Engine. *Intercontinental Geoinformation Days 5*. 2022; 112-115.
8. Li X, Wang N, Wu Y. Automated glacier snow line altitude calculation method using Landsat series images in Google Earth Engine platform. *Remote Sensing*. 2022; 14: 2377.
9. Zhang Q, Zhang Z, Wang X, et al. Monitoring of glacier area changes in the Ili River Basin during 1992–2020 based on Google Earth Engine. *Land*. 2024; 13: 1417.
10. Banerjee P. Long-term monitoring and forecasting of glacial lake dynamics using Landsat time series data, Google Earth Engine, machine learning, and geospatial analysis. *Discover Geoscience*. 2025; 3: 159.
11. Dou X, Fan X, Wang X, et al. Spatio-temporal evolution of glacial lakes in the Tibetan Plateau over the past 30 years. *Remote Sensing*. 2023; 15: 416.
12. Ahmad S, Jasrotia AS. Multi-decadal mapping of debris-covered glaciers in the Zaskar Himalaya using Landsat time series on Google Earth Engine. *J. Earth Syst. Sci*. 2026; 135: 64.
13. Sahu R, Ramsankaran RAAJ, Bhambri R, et al. Evolution of supraglacial lakes from 1990 to 2020 in the Himalaya–Karakoram region using cloud-based Google Earth Engine platform. *Journal of the Indian Society of Remote Sensing*. 2023; 51: 2379-2390.
14. Singh DK, Singh kk, Petropoulos GP, et al. Spatiotemporal vegetation variability and linkage with snow-hydroclimatic factors in Western Himalaya using remote sensing and Google Earth Engine. *Remote Sensing*. 2023; 15: 5239.
15. Ali A, Dunlop P, Coleman S, et al. Glacier area changes in Novaya Zemlya from 1986–89 to 2019–21 using object-based image analysis in Google Earth Engine. *Journal of Glaciology*. 2023; 69: 1305-1316.
16. Ortiz Diaz I, Lenzano MG, Araneo D. Temporal estimation of snow line altitude in glaciers of the Southern Patagonian Icefield using Google Earth Engine. *International Archives of the Photogrammetry, Remote Sensing and Spatial Information Sciences*. 2024; 48: 19-24.
17. Wang N, Zhong T, Zheng J, et al. Spatio-temporal distribution characteristics of glacial lakes in the Altai Mountains with climate change from 2000 to 2020. *Remote Sensing*. 2023; 15: 3689.
18. Cheng X, Shangguan D, Yang C, et al. Temporal and spatial changes of glacial lakes in the central Himalayas and their response to climate change based on multi-source remote sensing data. *Global and Planetary Change*. 2025; 245: 104675.
19. Gaddam VK, Ele SL, Bhandari S, et al. Applications of machine learning algorithms via Google Earth Engine interface to interpret snowline altitudes: A case study in Chandra Basin. In *International Conference on River Corridor Research and management*. Springer. 2023; 243-264.
20. Halder S, Bose S. Sustainable flood hazard mapping with GLOF: A Google Earth Engine approach. *Natural Hazards Research*. 2024; 4: 573-578.
21. Chen R, Yang H, Yang G, et al. Land-use mapping with multi-temporal Sentinel images based on Google Earth Engine in Southern Xinjiang Uygur Autonomous Region, China. *Remote Sensing*. 2023; 15: 3958.
22. Moazzam MFU, Banerjee A, Rahman G, et al. Elevation-dependent climate assessment and its influence on snow cover variability in Hindu Kush Himalayan region using Google Earth Engine for the period 2003–2021. *Remote Sensing Applications: Society and Environment*. 2024; 35: 101217.
23. Ray A, Raavi S, Gaddam VK, et al. Leveraging machine learning and Google Earth Engine for snowline altitude analysis: Insights from the Parbati Basin, India. *International Journal of Geoinformatics*. 2024; 20: 54-70.

-
24. de Almeida CR, Garcia N, Campos JC, et al. Time-series analyses of land surface temperature changes with Google Earth Engine in a mountainous region. *Heliyon*. 2023; 9: 18846.
 25. Melón-Nava A. Recent patterns and trends of snow cover (2000–2023) in the Cantabrian Mountains (Spain) from satellite imagery using Google Earth Engine. *Remote Sensing*. 2024; 16: 3592.
 26. Ahmad S, Jasrotia AS. Multi-decadal mapping of debris-covered glaciers in the Zaskar Himalaya using Landsat time series on Google Earth Engine. *J. Earth Syst. Sci.* 2026; 135: 64.
 27. Kumar R, Vijay S. Automated satellite-based glacial lake inventory and change detection in High Mountain Asia. *Scientific Reports*. 2026; 16.
 28. Parvin S, Irannezhad M, Marttila H, et al. MODIS-based assessment of snow cover variability in Iran's mountain ranges via Google Earth Engine. 2026.
 29. Chauhan P, Ngangom M. Spatio-temporal analysis of climate-induced multi-hazards in Ladakh using geospatial techniques. *Discover Geoscience*. 2026; 4: 100.
 30. Liu H, Wang D, Li T, et al. Glacier boundary extraction and spatiotemporal variation analysis in Geladandong region. *PeerJ*. 2026; 14: e20804.
 31. Dong Y, Chang X. Spatio-temporal analysis of land use and land cover changes: assessing urban expansion and ecological transformations (2003–2023). *Geo Journal*. 2026; 91: 40.
 32. El-Mahdy MES, El-Abd WA, Al-Metwaly WM, et al. Modeling flood dynamics in the Sudd wetlands using Google Earth Engine and AI models optimized with metaheuristics in a changing climate. *Journal of Water and Climate Change*. 2026; 17: 637-669.
 33. Yin M, Li A, Wang S, et al. X. Spatio-temporal variations in China's groundwater reservoirs from 2005 to 2024 based on GRACE data. *Sustainability*. 2026; 18: 2797.
 34. Huang X, Liu X, Du H, et al. STAGCNet: a change-aware dual-branch spatio-temporal fusion network for multitemporal land use/land cover classification. *Journal of Applied Remote Sensing*. 2026; 20: 021413-021413.
 35. Liu J, Li M, Shalamzari MJ, et al. A remote sensing-based early warning system for desertification: monitoring spatiotemporal dynamics and identifying risk zones. *Land Degradation & Development*. 2026.